Orthogonal Multiple Access Over Time- and Frequency-Selective Channels

Geert Leus, *Member, IEEE*, Shengli Zhou, *Member, IEEE*, and Georgios B. Giannakis, *Fellow, IEEE*

***Abstract*—Suppression of multiuser interference (MUI) and mitigation of time- and frequency-selective (doubly selective) channel effects constitute major challenges in the design of third-generation wireless mobile systems. Relying on a basis expansion model (BEM) for doubly selective channels, we develop a channel-independent block spreading scheme that preserves mutual orthogonality among single-cell users at the receiver. This alleviates the need for complex multiuser detection, and enables separation of the desired user by a simple code-matched channel-independent block despreading scheme that is maximum-likelihood (ML) optimal under the BEM plus white Gaussian noise assumption on the channel. In addition, each user achieves the maximum delay-Doppler diversity for Gaussian distributed BEM coefficients. Issues like links with existing multiuser transceivers, existence, user efficiency, special cases, backward compatibility with direct-sequence code-division multiple access (DS-CDMA), and error control coding, are briefly discussed.**

***Index Terms*—Delay diversity, Doppler diversity, multiple access, multiuser detection, time- and frequency-selective channels.**

I. Introduction

RELYING on a finite impulse response (FIR) model for frequency-selective channels, several channel-independent block spreading schemes have recently been developed that preserve mutual orthogonality among users at the receiver [7], [10], [24], [27]. This orthogonality enables separation of the desired user by a simple code-matched channel-independent block despreading scheme that is maximum-likelihood (ML) optimal under the FIR plus white Gaussian noise assumption on the channel. Moreover, each user achieves the maximum delay diversity for Gaussian distributed FIR model coefficients. These transceivers serve as attractive alternatives to the multiuser RAKE receiver for direct-sequence code-division multiple access (DS-CDMA) proposed in [28] (see also [23]), which does not achieve the maximum delay diversity gain, and requires knowledge of the spreading codes of all active users for detection. All these transceivers, however, are based on the key assumption that the underlying channels are time invariant over the transmitted block. In practical scenarios, this assumption does not hold true when channel time-variation arises due to high mobility, carrier frequency offsets, and phase drifts.

In this paper, we deal with doubly selective (time- and frequency-selective) channels. We rely on a basis expansion model (BEM) for doubly-selective channels, which incorporates time-variation explicitly. The BEM has previously been used in [15], and has been extended to include the space dimension in [13]. Note that the models in [15], [13] fit within the framework of the more general BEM introduced in [22], [6]. Relying on this BEM for doubly selective channels, we then develop a channel-independent block spreading scheme that preserves mutual orthogonality among users at the receiver. This orthogonality enables separation of the desired user by a simple code-matched channel-independent block despreading scheme that is ML optimal under the BEM plus white Gaussian noise assumption on the channel. Moreover, each user achieves the maximum delay-Doppler diversity for Gaussian distributed BEM coefficients. This transceiver serves as an attractive alternative to the multiuser time-frequency RAKE receivers for DS-CDMA proposed in [16], which does not achieve the maximum delay-Doppler diversity gain, and requires the knowledge of the spreading codes of all active users for detection.

We also briefly discuss some interesting issues related to the proposed transceiver, such as links with existing multiuser transceivers, existence, user efficiency, special cases, backward compatibility with DS-CDMA, and error control coding.

The rest of this paper is organized as follows. In Section II, we discuss the wireless doubly selective channel and introduce the BEM for such a channel. Based on this BEM, a data model is described in Section III. The proposed transceiver is developed in detail in Section IV. In Section V, we discuss some interesting issues related to the proposed transceiver. Conclusions are finally presented in Section VI.

Notation: We use upper (lower) bold face letters to denote matrices (column vectors). $(\cdot)^*$, $(\cdot)^T$, and $(\cdot)^H$ represent conjugate, transpose, and Hermitian, respectively. The set of real and integer numbers are defined as $\mathbb{R}$ and $\mathbb{Z}$, respectively. The set of nonnegative real numbers is defined as $\mathbb{R}_0^+$, and the set of positive real numbers as $\mathbb{R}^+$. Similarly, the set of nonnegative integer numbers is defined as $\mathbb{Z}_0^+$, and the set of positive integer numbers as $\mathbb{Z}^+$. We reserve $\mathrm{E}\{\cdot\}$ for expectation, $\|\cdot\|$ for Frobenius norm, $\lfloor\cdot\rfloor$ for integer flooring, and $\lceil\cdot\rceil$ for integer ceiling. The Kronecker delta is denoted as $\delta[\cdot]$. We define $\otimes$ as the Kronecker product, and $\star$ as the convolution. The $M \times N$ all-zero matrix is denoted as $\mathbf{0}_{M\times N}$, the $N \times N$ identity matrix as $\boldsymbol{I}_N$,

Manuscript received July 2, 2001; revised January 28, 2003. This work was supported by the FWO–Flanders (Belgium), the ARL/CTA under Grant DAAD19-01-2-011, and the National Science Foundation Wireless Initiative under Grant ECS-9979443. The material in this paper was presented in part at the 35th Asilomar Conference on Signals, Systems, and Computers, Pacific Grove, CA, November 2001 and at IEEE GLOBECOM, San Antonio, TX, November 2001.

G. Leus is with the Department of Electrical Engineering (ESAT), Katholieke Universiteit Leuven, B-3001 Haverlee, Belgium (e-mail: geert.leus@ esat.kuleuven.ac.be).

S. Zhou and G. B. Giannakis are with the Department of Electrical and Computer Engineering, University of Minnesota, Minneapolis, MN 55455 USA (e-mail: szhou@ece.umn.edu; georgios@ece.umn.edu).

Communicated by V. V. Veeravalli, Associate Editor for Detection and Estimation.

Digital Object Identifier 10.1109/TIT.2003.814477

and the $N \times N$ unitary fast Fourier transform (FFT) matrix as $\boldsymbol{F}_N$. We define $\boldsymbol{i}_N[n]$ as the $(n+1)$th column of $\boldsymbol{I}_N$, and $\boldsymbol{f}_N[n]$ as the $(n+1)$th column of $\boldsymbol{F}_N$. Furthermore, we define

$$\boldsymbol{f}_N(\nu) := [1, \exp(j2\pi\nu), \ldots, \exp(j2\pi(N-1)\nu)]^T$$

and $\boldsymbol{\Lambda}_N(\nu)$ as the $N \times N$ diagonal matrix with main diagonal $\boldsymbol{f}_N(\nu)$. Finally, we define $[\boldsymbol{A}]_{m,n}$ as the $(m+1, n+1)$th entry of the matrix $\boldsymbol{A}$, and $[\boldsymbol{a}]_n$ as the $(n+1)$th entry of the vector $\boldsymbol{a}$.

II. Wireless Doubly Selective Channel

Suppose the uth user's $(u \in \{0, \ldots, U-1\})$ symbol sequence $s_u[m]$ is somehow converted into a chip sequence $x_u[n]$ that is to be transmitted with chip period T. For the proposed design, this will be discussed in Section III. Focusing on a baseband description, this chip stream $x_u[n]$ is filtered at the transmitter by $h^{\rm tr}(t)$, distorted by the physical channel $h_u^{\rm ch}(t;\tau)$, corrupted by the additive noise $\zeta(t)$, and finally filtered at the receiver by $h^{\rm rec}(t)$. The aggregate received signal $y(t)$ from all users can then be written as

$$y(t) = \sum_{u=0}^{U-1} \sum_{n=-\infty}^{\infty} h_u(t; t-nT) x_u[n] + \eta(t)$$

where $\eta(t) := g^{\rm rec}(t) \star \zeta(t)$, and [5, Ch. 1]

$$h_u(t;\tau) := \int_{-\infty}^{\infty}\int_{-\infty}^{\infty} h^{\rm rec}(s) h^{\rm tr}(\tau-\theta-s) h_u^{\rm ch}(t-s;\theta)\, ds\, d\theta. \tag{1}$$

With chip rate sampling, the received sequence $y[n] := y(nT)$ can now be written as

$$y[n] = \sum_{u=0}^{U-1} \sum_{\nu=-\infty}^{\infty} h_u[n;\nu] x_u[n-\nu] + \eta[n] \tag{2}$$

where $\eta[n] := \eta(nT)$, and $h_u[n;\nu] := h_u(nT;\nu T)$. Note that when $h^{\rm rec}(t)$ has square-root Nyquist characteristics, the whiteness of the noise is preserved after chip rate sampling.

General models to describe $h_u[n;\nu]$ usually contain many parameters [8, Ch. 1], [3, Ch. 3], [4], [5, Ch. 1]. That is why we want to use a simpler model to describe $h_u[n;\nu]$ with less parameters. Let us first introduce the following assumptions:

A1) the maximum lag offset of $h_u^{\rm ch}(t;\tau)$ is bounded by $\tau_{\max}$;

A2) the maximum absolute frequency offset of $h_u^{\rm ch}(t;\tau)$ is bounded by $f_{\max}$;

where $\tau_{\max}$ and $f_{\max}$ are referred to as the delay and Doppler spread, respectively. Both A1) and A2) can be satisfied in practice, in both uplink and downlink operations, without the need for *stringent* timing and carrier frequency synchronization. If we then design a quadruple (T, N, L, Q) with $T \in \mathbb{R}^+$, $N \in \mathbb{Z}^+$, and $L, Q \in \mathbb{Z}_0^+$, that satisfies the following conditions:

C1) $LT \geq \tau_{\max}$;

C2) $Q/(NT) \geq f_{\max}$;

the channel $h_u[n;\nu]$ can be accurately described by the following BEM for doubly selective channels:

$$h_u[n;\nu] = \sum_{l=0}^{L} \delta[\nu-l] \sum_{q=-Q}^{Q} h_{u,q}[\lfloor n/N \rfloor; l] e^{j2\pi qn/N} \tag{3}$$

where L represents the (discrete) delay spread (i.e., the delay spread in multiples of the time-domain resolution T), and Q represents the (discrete) Doppler spread (i.e., the Doppler spread expressed in multiples of the frequency-domain resolution $1/(NT)$). Notice that in every block of N chip periods, a new realization of the BEM is considered, with new BEM coefficients $\{\{h_{u,q}[i;l]\}_{l=0}^{L}\}_{q=-Q}^{Q}$.

The BEM of (3) is not new. It has previously been used in [15], and has been extended to include the space dimension in [13]. Further note that the BEM of (3) fits within the framework of the more general BEM introduced in [22], [6]. In addition, a BEM using wavelet basis functions has been studied in [12].

III. Data Model

We start from the design of a quadruple (T, N, L, Q) that satisfies conditions C1) and C2). Similar to multicode CDMA, we use *block spreading* to convert the uth user's symbol stream $s_u[m]$ into a chip stream $x_u[n]$. The symbol sequence $s_u[m]$ is first serial-to-parallel converted into a sequence of $M \times 1$ symbol blocks

$$\boldsymbol{s}_u[i] := [s_u[iM], \ldots, s_u[(i+1)M-1]]^T.$$

Each symbol block $\boldsymbol{s}_u[i]$ is then spread by an $N \times M$ spreading matrix $\boldsymbol{C}_u$ to obtain a sequence of $N \times 1$ chip blocks $\boldsymbol{x}_u[i] := \boldsymbol{C}_u \boldsymbol{s}_u[i]$. This sequence of chip blocks $\boldsymbol{x}_u[i]$ is finally parallel-to-serial converted into a chip sequence $x_u[n]$. With chip rate sampling, the received sequence $y[n]$ can then be written as (2), where $h_u[n;\nu]$ is given by (3). The use of the BEM of (3) is justified because the quadruple (T, N, L, Q) is chosen to satisfy conditions C1) and C2).

At the receiver, we serial-to-parallel convert the received sequence $y[n]$ into a sequence of received blocks

$$\boldsymbol{y}[i] := [y[iN], \ldots, y[(i+1)N-1]]^T$$

which can be written as

$$\boldsymbol{y}[i] = \sum_{u=0}^{U-1} \sum_{a=0}^{\lceil L/N \rceil} \sum_{q=-Q}^{Q} \boldsymbol{\Lambda}_N\left(\frac{q}{N}\right) \boldsymbol{H}_{N,u,q}^{(a)}[i] \boldsymbol{C}_u \boldsymbol{s}_u[i-a] + \boldsymbol{\eta}[i] \tag{4}$$

where $\boldsymbol{\eta}[i] := [\eta[iN], \ldots, \eta[(i+1)N-1]]^T$ and $\boldsymbol{H}_{N,u,q}^{(a)}[i]$ represents the $N \times N$ Toeplitz matrix with

$$[\boldsymbol{H}_{N,u,q}^{(a)}[i]]_{n,n'} = h_{u,q}[i; n-n'+aN].$$

Remember that $\boldsymbol{\Lambda}_N(\nu)$ has been defined as the $N \times N$ diagonal matrix with main diagonal $\boldsymbol{f}_N(\nu)$. Note that $\lceil L/N \rceil + 1$ symbol blocks $\boldsymbol{s}_u[i]$ contribute to each received block $\boldsymbol{y}[i]$; the terms with $a > 1$ represent the so-called interblock interference (IBI). This IBI can be avoided by designing $\boldsymbol{C}_u$ to have $N > L$, while selecting its L last rows to be zero. We then obtain the following IBI-free model:

$$\boldsymbol{y}[i] = \sum_{u=0}^{U-1} \sum_{q=-Q}^{Q} \boldsymbol{\Lambda}_N \left(\frac{q}{N}\right) \boldsymbol{H}_{N,u,q}^{(0)}[i] \boldsymbol{C}_u \boldsymbol{s}_u[i] + \boldsymbol{\eta}[i]. \quad (5)$$

Defining the uth user's equivalent $N \times M$ spreading matrix seen at the receiver as

$$\overline{\boldsymbol{C}}_u[i] := \sum_{q=-Q}^{Q} \boldsymbol{\Lambda}_N \left(\frac{q}{N}\right) \boldsymbol{H}_{N,u,q}^{(0)}[i] \boldsymbol{C}_u$$

this channel input–output relationship can be expressed as

$$\boldsymbol{y}[i] = \sum_{u=0}^{U-1} \overline{\boldsymbol{C}}_u[i] \boldsymbol{s}_u[i] + \boldsymbol{\eta}[i].$$

IV. Orthogonal Multiple Access

The goal of this paper is to design a channel-independent block spreading scheme that preserves mutual orthogonality among users *even after* propagation through any doubly selective BEM channel. In other words, we want to design a spreading matrix $\boldsymbol{C}_u$ that is independent of the BEM realization, and possesses mutual orthogonality among users; i.e., $\boldsymbol{C}_u^H \boldsymbol{C}_{u'} = \boldsymbol{0}_{M\times M}, \forall\, u \neq u'$, such that the equivalent spreading matrix seen at the receiver $\overline{\boldsymbol{C}}_u[i]$ also possesses mutual orthogonality among users; i.e., $\overline{\boldsymbol{C}}_u^H[i] \overline{\boldsymbol{C}}_{u'}[i] = \boldsymbol{0}_{M\times M}, \forall\, u \neq u'$, regardless of the BEM realization. This alleviates the need for complex multiuser detection, and enables separation of the desired user by a simple code-matched channel-independent block despreading scheme that is ML optimal under the BEM plus white Gaussian noise assumption on the channel. On the single-user output obtained after block despreading, one can then apply any single-user equalizer to mitigate intersymbol interference (ISI).

In addition to preserving mutual orthogonality among users after propagation through any doubly selective BEM channel, we wish our spreading matrices to enable the maximum delay-Doppler diversity per user, when the BEM coefficients are Gaussian distributed.

A. Block Spreading Design

Suppose the quadruple (T, N, L, Q) was designed in such a way that we can find two new parameters $K, P \in \mathbb{Z}^+$ that satisfy the following condition:

C3) $N = U(P+2Q)(K+L)$.

As symbol block length we then take $M = PK$. We further assign to each user u a distinct $U \times 1$ code vector $\boldsymbol{c}_u$. We select the code vectors $\{\boldsymbol{c}_u\}_{u=0}^{U-1}$ to be mutually orthogonal with unit norm, i.e., $\boldsymbol{c}_u^H \boldsymbol{c}_{u'} = \delta[u-u']$. The $N \times M$ spreading matrix $\boldsymbol{C}_u$ is then designed as

$$\boldsymbol{C}_u = \left[\boldsymbol{F}_{U(P+2Q)}^H (\boldsymbol{c}_u \otimes \boldsymbol{T}_2)\right] \otimes \boldsymbol{T}_1 \quad (6)$$

where $\boldsymbol{T}_1$ is the $(K+L) \times K$ zero-padding matrix defined as $\boldsymbol{T}_1 := [\boldsymbol{I}_K, \boldsymbol{0}_{K\times L}]^T$, and $\boldsymbol{T}_2$ is the $(P+2Q) \times P$ two-sided zero-inserting matrix defined as $\boldsymbol{T}_2 := [\boldsymbol{0}_{P\times Q}, \boldsymbol{I}_P, \boldsymbol{0}_{P\times Q}]^T$. First, note that the $\boldsymbol{C}_u$ of (6) is designed to have $N > L$, as per C3), while its L last rows are selected to be zero, and thus IBI is avoided. It is further clear that the $\boldsymbol{C}_u$ in (6) is independent of the BEM realization, and possesses mutual orthogonality among users, i.e., $\boldsymbol{C}_u^H \boldsymbol{C}_{u'} = \boldsymbol{0}_{M\times M}, \forall\, u \neq u'$. The latter is due to the fact that the code vectors $\{\boldsymbol{c}_u\}_{u=0}^{U-1}$ are selected to be mutually orthogonal, and can easily be proven using the rule for the product of Kronecker products of matrices with matching dimensions [2]

$$(\boldsymbol{A}_1 \otimes \boldsymbol{A}_2)(\boldsymbol{A}_3 \otimes \boldsymbol{A}_4) = (\boldsymbol{A}_1\boldsymbol{A}_3) \otimes (\boldsymbol{A}_2\boldsymbol{A}_4)$$

and the corresponding Hermitian property of Kronecker products [2]

$$(\boldsymbol{A}_1 \otimes \boldsymbol{A}_2)^H = \boldsymbol{A}_1^H \otimes \boldsymbol{A}_2^H.$$

These two rules are used repeatedly throughout this paper. What remains to be shown is that the equivalent spreading matrix seen at the receiver, $\overline{\boldsymbol{C}}_u[i]$, also possesses mutual orthogonality among users, i.e., $\overline{\boldsymbol{C}}_u^H[i] \overline{\boldsymbol{C}}_{u'}[i] = \boldsymbol{0}_{M\times M}, \forall\, u \neq u'$, regardless of the BEM realization. This is shown in the next proposition.

Proposition 1: When $\boldsymbol{C}_u$ is designed as in (6), the equivalent spreading matrix seen at the receiver $\overline{\boldsymbol{C}}_u[i]$ possesses mutual orthogonality among users, i.e., $\overline{\boldsymbol{C}}_u^H[i] \overline{\boldsymbol{C}}_{u'}[i] = \boldsymbol{0}_{M\times M}$, $\forall\, u \neq u'$, regardless of the BEM realization. More specifically, introducing the notation $\boldsymbol{J}_{N,q}^{(a)}$ to represent the $N \times N$ shift (Toeplitz) matrix with $[\boldsymbol{J}_{N,q}^{(a)}]_{n,n'} = \delta[n - n' - q + aN]$, and defining the matrices

$$\boldsymbol{H}_{u,q}[i] := \boldsymbol{H}_{K+L,u,q}^{(0)}[i] \boldsymbol{T}_1$$
$$\boldsymbol{\Delta}_q := \boldsymbol{\Lambda}_{K+L}\left(\frac{q}{N}\right)$$
$$\boldsymbol{J}_q := \boldsymbol{J}_{P+2Q,q}^{(0)} \boldsymbol{T}_2$$

the equivalent spreading matrix seen at the receiver can be written as

$$\overline{\boldsymbol{C}}_u[i] = \sum_{q=-Q}^{Q} \boldsymbol{\Lambda}_N \left(\frac{q}{N}\right) \boldsymbol{H}_{N,u,q}^{(0)}[i] \boldsymbol{C}_u = \boldsymbol{D}_u \boldsymbol{\mathcal{H}}_u[i] \quad (7)$$

where $\boldsymbol{D}_u$ is the $N \times (P+2Q)(K+L)$ matrix given by

$$\boldsymbol{D}_u := \left[\boldsymbol{F}_{U(P+2Q)}^H (\boldsymbol{c}_u \otimes \boldsymbol{I}_{P+2Q})\right] \otimes \boldsymbol{I}_{K+L}, \quad (8)$$

and $\boldsymbol{\mathcal{H}}_u[i]$ is the $(P+2Q)(K+L) \times M$ matrix given by

$$\boldsymbol{\mathcal{H}}_u[i] := \sum_{q=-Q}^{Q} \boldsymbol{J}_q \otimes (\boldsymbol{\Delta}_q \boldsymbol{H}_{u,q}[i]) = \begin{bmatrix} \boldsymbol{\Delta}_{-Q}\boldsymbol{H}_{u,-Q}[i] & & \\ \vdots & \ddots & \\ \boldsymbol{\Delta}_Q \boldsymbol{H}_{u,Q}[i] & & \boldsymbol{\Delta}_{-Q} H_{u,-Q}[i] \\ & \ddots & \vdots \\ & & \boldsymbol{\Delta}_Q \boldsymbol{H}_{u,Q}[i] \end{bmatrix}. \quad (9)$$

Proof: We first prove that (7) holds true. In Appendixes A and B, we prove the following equalities:

$$\boldsymbol{H}_{N,u,q}^{(0)}[i] \boldsymbol{C}_u = \left\{\left[\boldsymbol{F}_{U(P+2Q)}^H (\boldsymbol{c}_u \otimes \boldsymbol{T}_2)\right] \otimes \boldsymbol{I}_{K+L}\right\} (\boldsymbol{I}_P \otimes \boldsymbol{H}_{u,q}[i]) \quad (10)$$

$$\boldsymbol{\Lambda}_N\left(\frac{q}{N}\right) \left\{\left[\boldsymbol{F}_{U(P+2Q)}^H (\boldsymbol{c}_u \otimes \boldsymbol{T}_2)\right] \otimes \boldsymbol{I}_{K+L}\right\} = \boldsymbol{D}_u (\boldsymbol{J}_q \otimes \boldsymbol{\Delta}_q) \quad (11)$$

with $\boldsymbol{C}_u$ and $\boldsymbol{D}_u$ defined in (6) and (8), respectively. From (10) and (11), we then obtain

$$\begin{aligned}\overline{\boldsymbol{C}}_u[i] &= \sum_{q=-Q}^{Q} \boldsymbol{\Lambda}_N\left(\frac{q}{N}\right)\boldsymbol{H}^{(0)}_{N,u,q}[i]\boldsymbol{C}_u \\ &= \boldsymbol{D}_u\left\{\sum_{q=-Q}^{Q}(\boldsymbol{J}_q\otimes\boldsymbol{\Delta}_q)(\boldsymbol{I}_P\otimes\boldsymbol{H}_{u,q}[i])\right\} \\ &= \boldsymbol{D}_u\left\{\sum_{q=-Q}^{Q}\boldsymbol{J}_q\otimes(\boldsymbol{\Delta}_q\boldsymbol{H}_{u,q}[i])\right\} \\ &= \boldsymbol{D}_u\boldsymbol{\mathcal{H}}_u[i]. \end{aligned} \tag{12}$$

From the fact that $\boldsymbol{D}_u$ possesses mutual orthogonality among users, i.e.,

$$\boldsymbol{D}_u^H\boldsymbol{D}_{u'} = \boldsymbol{0}_{(P+2Q)(K+L)\times(P+2Q)(K+L)}, \qquad \forall u \neq u'$$

and $\overline{\boldsymbol{C}}_u[i]$ falls in the column space of $\boldsymbol{D}_u$, it follows that $\overline{\boldsymbol{C}}_u^H[i]\overline{\boldsymbol{C}}_{u'}[i] = \boldsymbol{0}_{M\times M}$, $\forall u \neq u'$, regardless of the BEM realization. This concludes the proof. □

B. Block Despreading Design

Thanks to our special block spreading design that preserves mutual orthogonality among users after propagation through any doubly selective BEM channel, the desired user can be separated using a code-matched channel-independent block despreading scheme that is ML optimal under the BEM plus white Gaussian noise assumption on the channel. Indeed, if we despread $\boldsymbol{y}[i]$ by the $N\times(P+2Q)(K+L)$ despreading matrix $\boldsymbol{D}_u$, we can extract the uth user, to obtain

$$\overline{\boldsymbol{y}}_u[i] = \boldsymbol{D}_u^H\boldsymbol{y}[i] = \boldsymbol{\mathcal{H}}_u[i]\boldsymbol{s}_u[i] + \overline{\boldsymbol{\eta}}_u[i] \tag{13}$$

where $\overline{\boldsymbol{\eta}}_u[i] := \boldsymbol{D}_u^H\boldsymbol{\eta}[i]$. Notice that $\boldsymbol{D}_u$ is independent of the BEM realization. More specifically, it only depends on the code vector $\boldsymbol{c}_u$ assigned to the uth user, and thus performs a code-matched filtering. Moreover, since $\overline{\boldsymbol{C}}_u[i]$ falls in the column space of $\boldsymbol{D}_u$, and $\boldsymbol{D}_u$ is a tall unitary matrix, i.e., $\boldsymbol{D}_u^H\boldsymbol{D}_u = \boldsymbol{I}_{(P+2Q)(K+L)}$, which means it does not color $\boldsymbol{\eta}[i]$, the block despreading is ML optimal under the BEM plus white Gaussian noise assumption on the channel. Hence, in the presence of additive white Gaussian noise $\boldsymbol{\eta}[i]$, a multiuser detection problem has been converted without loss of ML optimality into a set of single-user equalization problems, as depicted in Fig. 1.

On the single-user output $\overline{\boldsymbol{y}}_u[i]$, we can then apply any single-user equalizer to mitigate the ISI. We can, e.g., adopt the linear zero-forcing (ZF) equalizer given by

$$\boldsymbol{\Gamma}_u^{\mathrm{zf}}[i] := (\boldsymbol{\mathcal{H}}_u^H[i]\boldsymbol{R}_{u,\overline{\eta}}^{-1}\boldsymbol{\mathcal{H}}_u[i])^{-1}\boldsymbol{\mathcal{H}}_u^H[i]\boldsymbol{R}_{u,\overline{\eta}}^{-1}$$

or the linear minimum mean-squared error (MMSE) equalizer given by

$$\boldsymbol{\Gamma}_u^{\mathrm{mmse}}[i] := (\boldsymbol{\mathcal{H}}_u^H[i]\boldsymbol{R}_{u,\overline{\eta}}^{-1}\boldsymbol{\mathcal{H}}_u[i] + \boldsymbol{R}_{u,s}^{-1})^{-1}\boldsymbol{\mathcal{H}}_u^H[i]\boldsymbol{R}_{u,\overline{\eta}}^{-1},$$

where

$$\boldsymbol{R}_{u,s} := \mathrm{E}\{\boldsymbol{s}_u[i]\boldsymbol{s}_u^H[i]\}$$

and

$$\boldsymbol{R}_{u,\overline{\eta}} := \mathrm{E}\{\overline{\boldsymbol{\eta}}_u[i]\overline{\boldsymbol{\eta}}_u^H[i]\}.$$

Nonlinear approaches including decision feedback equalization and near-ML equalization using sphere decoding can also be applied, but are beyond the scope of this paper. The block diagram of the proposed transceiver is depicted in Fig. 2.

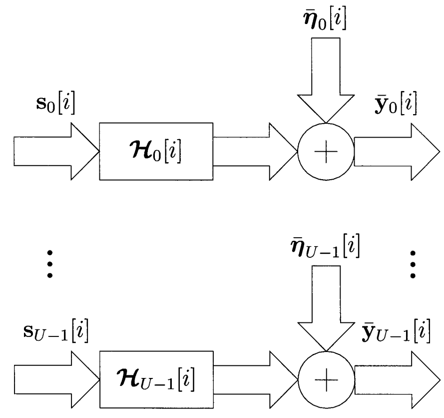

Fig. 1. Set of equivalent single-user equalization problems.

C. Enabling Maximum Delay-Doppler Diversity

We will establish here that on top of preserving mutual orthogonality among users after propagation through any doubly selective BEM channel, our spreading matrices are special in the sense that they enable the maximum delay-Doppler diversity per user, when the BEM coefficients are Gaussian distributed. The maximum delay-Doppler diversity for Gaussian distributed BEM coefficients is defined in [11] as $r_{u,h} := \mathrm{rank}\{\boldsymbol{R}_{u,h}\}$, where

$$\begin{aligned}\boldsymbol{R}_{u,h} &:= \mathrm{E}\{\boldsymbol{h}_u[i]\boldsymbol{h}_u^H[i]\} \\ \boldsymbol{h}_u[i] &:= [\boldsymbol{h}_{u,-Q}^T[i], \ldots, \boldsymbol{h}_{u,Q}^T[i]]^T\end{aligned}$$

and

$$\boldsymbol{h}_{u,q}[i] = [h_{u,q}[i;0], \ldots, h_{u,q}[i;L]]^T.$$

When $\boldsymbol{R}_{u,h}$ has full rank, the maximum delay-Doppler diversity is given by $r_{u,h,\max} = (2Q+1)(L+1)$, which is the number of degrees of freedom in the BEM.

Proposition 2: The block spreading in the single-user model (13) enables the maximum delay-Doppler diversity for Gaussian distributed BEM coefficients.

Proof: Denoting $\boldsymbol{e}_u[i] := \boldsymbol{s}_u[i] - \boldsymbol{s}'_u[i]$ as the error vector between the symbol blocks $\boldsymbol{s}_u[i]$ and $\boldsymbol{s}'_u[i]$, we can express the Euclidean distance between $\boldsymbol{z}_u[i] := \boldsymbol{\mathcal{H}}_u[i]\boldsymbol{s}_u[i]$ and $\boldsymbol{z}'_u[i] := \boldsymbol{\mathcal{H}}_u[i]\boldsymbol{s}'_u[i]$ as

$$\mathrm{d}\{\boldsymbol{z}_u[i], \boldsymbol{z}'_u[i]\} = \|\boldsymbol{\mathcal{H}}_u[i]\boldsymbol{e}_u[i]\| = \|\boldsymbol{\mathcal{E}}_u[i]\boldsymbol{h}_u[i]\| \tag{14}$$

where $\boldsymbol{\mathcal{E}}_u[i]$ is some $(P+2Q)(K+L)\times(2Q+1)(L+1)$ matrix that depends on $\boldsymbol{e}_u[i]$ (the exact form is not important). Computing the eigenvalue decomposition of $\boldsymbol{R}_{u,h}$ yields $\boldsymbol{R}_{u,h} = \boldsymbol{V}_u\boldsymbol{\Sigma}_u\boldsymbol{V}_u^H$, where $\boldsymbol{V}_u$ is a $(2Q+1)(L+1)\times r_{u,h}$ unitary matrix satisfying $\boldsymbol{V}_u^H\boldsymbol{V}_u = \boldsymbol{I}_{r_{u,h}}$, and $\boldsymbol{\Sigma}_u$ is an $r_{u,h}\times r_{u,h}$ diagonal matrix. From [11], we know that the block spreading in the single-user model (13) enables the maximum delay-Doppler diversity for Gaussian distributed BEM coefficients, if and only if the $r_{u,h}\times r_{u,h}$ matrix $\boldsymbol{A}_u := (\boldsymbol{V}_u\boldsymbol{\Sigma}_u^{1/2})^H\boldsymbol{\mathcal{E}}_u^H[i]\boldsymbol{\mathcal{E}}_u[i]\boldsymbol{V}_u\boldsymbol{\Sigma}_u^{1/2}$ has full rank $r_{u,h}$ for all $\boldsymbol{e}[i] \neq \boldsymbol{0}$. This is satisfied if $\boldsymbol{\mathcal{E}}_u^H[i]\boldsymbol{\mathcal{E}}_u[i]$ has full rank $(2Q+1)(L+1)$ for all $\boldsymbol{e}[i] \neq \boldsymbol{0}$. Since $\boldsymbol{\mathcal{E}}_u^H[i]\boldsymbol{\mathcal{E}}_u[i]$ is symmetric, having full rank is equivalent to being positive defi-

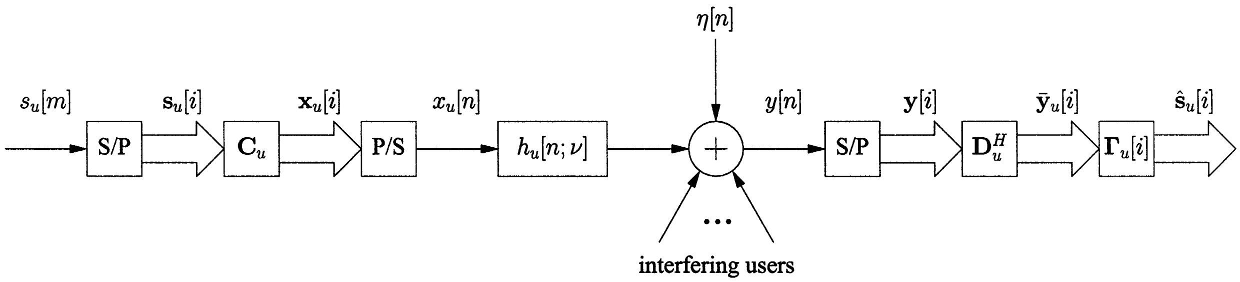

Fig. 2. Block diagram of the proposed transceiver (only the uth user shown).

nite. Hence, we require $\|\boldsymbol{\mathcal{E}}_u[i]\boldsymbol{h}_u[i]\| > 0$ for all $\boldsymbol{e}[i] \neq \mathbf{0}$, and for all $\boldsymbol{h}_u[i] \neq \mathbf{0}$. From (14), this corresponds to $\|\boldsymbol{\mathcal{H}}_u[i]\boldsymbol{e}_u[i]\| > 0$ for all $\boldsymbol{e}[i] \neq \mathbf{0}$, and for all $\boldsymbol{h}_u[i] \neq \mathbf{0}$. This is satisfied when $\boldsymbol{\mathcal{H}}_u[i]$ has full rank M for all $\boldsymbol{h}_u[i] \neq \mathbf{0}$. The latter is proven next.

Due to the tall upper triangular Toeplitz structure of $\boldsymbol{H}_{u,q}[i]$, with $h_{u,q}[i;\, l]$ on the lth diagonal, it is clear that $\boldsymbol{H}_{u,q}[i]$ has full column rank K for all $\boldsymbol{h}_{u,q}[i] \neq \mathbf{0}$. Hence, $\boldsymbol{\Delta}_q\boldsymbol{H}_{u,q}[i]$ also has full column rank K for all $\boldsymbol{h}_{u,q}[i] \neq \mathbf{0}$. If $\boldsymbol{h}_u[i] \neq \mathbf{0}$, then at least one vector $\boldsymbol{h}_{u,q}[i] \neq \mathbf{0}$, and thus at least one matrix $\boldsymbol{\Delta}_q\boldsymbol{H}_{u,q}[i]$ has full column rank K. Due to the tall upper triangular Toeplitz block structure of $\boldsymbol{\mathcal{H}}_u[i]$, with $\boldsymbol{\Delta}_q\boldsymbol{H}_{u,q}[i]$ on the qth block diagonal, it is then clear that $\boldsymbol{\mathcal{H}}_u[i]$ has full column rank M for all $\boldsymbol{h}_u[i] \neq \mathbf{0}$. This statement concludes the proof. □

Note that $\boldsymbol{\mathcal{H}}_u[i]$ having full rank M for all $\boldsymbol{h}_u[i] \neq \mathbf{0}$ means that the symbols are guaranteed to be detectable in the absence of noise, regardless of the BEM realization. This is in contrast with DS-CDMA, where the signature sequences from different users may become linearly dependent after propagation through a nonflat channel (see [5, Ch. 6] for an illustrative example). This is also the reason why multiuser detection methods for DS-CDMA over nonflat channels do not ensure the maximum diversity.

D. Numerical Example

To illustrate the performance of the proposed transceiver, let us consider a small numerical example. We consider the same fading scenario as in [16], and compare the proposed transceiver with the multiuser time–frequency RAKE receiver for DS-CDMA proposed in [16]. As in [16], we take $N = 63$, $L = 1$, $Q = 1$, and generate a set of independent channels $\{h_u[n;\,\nu]\}_{u=0}^{U-1}$ (c.f. (3)) with $h_{u,q}[i;\, l]$ complex Gaussian distributed with variance 0.9 if $q = 0$, and 0.05 if $q = \pm 1$. We assume here that the receiver knows the channels $\{h_u[n;\,\nu]\}_{u=0}^{U-1}$. For the proposed transceiver, N corresponds to the length of the transmitted chip block, while for the multiuser time–frequency RAKE receiver for DS-CDMA, N corresponds to the spreading gain. In order to satisfy condition C3), the proposed transceiver uses $U = 7$, $P = 1$, and $K = 2$. Assuming binary phase-shift keying (BPSK) modulation, note that in the $N = 63$ chip periods, the proposed transceiver can handle 2 bits per user ($M = PK = 2$), while the multiuser time–frequency RAKE receiver for DS-CDMA can only handle 1 bit per user. Keeping this important rate difference in mind, Fig. 3 depicts a comparison between the performance of the proposed transceiver with linear ZF equalization, and the performance of the linear ZF multiuser time–frequency RAKE receiver for DS-CDMA (the latter performance corresponds to the one shown in [16, Fig. 3]). Note that the signal-to-noise ratio (SNR) per user is defined as the ensemble average received bit energy per user over the noise variance. From Fig. 3, we observe that the performance of the proposed transceiver accommodating seven users (that transmit 2 bits/63 chips) is comparable to the performance of the multiuser time–frequency RAKE receiver for DS-CDMA accommodating only two users (that transmit 1 bit/63 chips), and much better than the performance of the multiuser time–frequency RAKE receiver for DS-CDMA accommodating seven users (that transmit 1 bit/63 chips). More specifically, with seven users we gain about 4 dB for a bit-error rate (BER) of 10^{-3}.

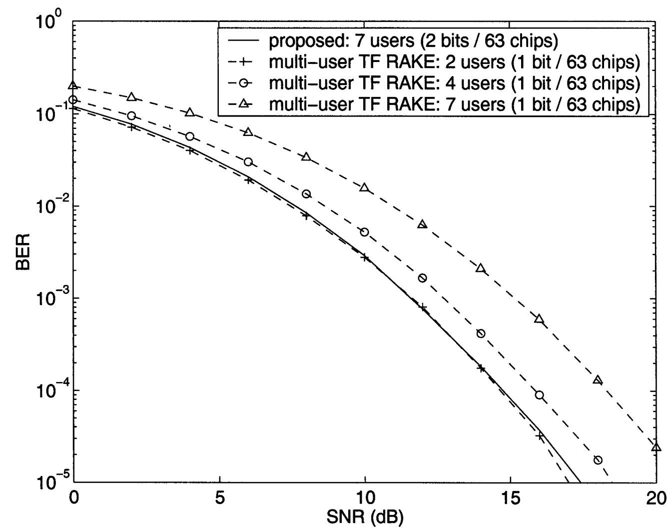

Fig. 3. Average BER versus SNR per user; comparison between the proposed transceiver and the multiuser time–frequency RAKE receiver for DS-CDMA.

V. Further Discussions

In this section, we briefly discuss some interesting issues related to the proposed transceiver, such as links with existing multiuser transceivers, existence, user efficiency, special cases, backward compatibility with DS-CDMA, and error control coding.

Links With Existing Multiuser Transceivers: Existing multiuser transceivers for doubly selective channels also make use of the BEM of (3), but either rely on spatial-division multiple access (SDMA) [20], [21], or, on DS-CDMA combined with multiuser detection [16] to separate the users.[1] As our

[1]Spread-signature DS-CDMA [25], [26] over doubly selective channels has been discussed in [1].

scheme, all these schemes start from the design of a quadruple (T, N, L, Q) that satisfies conditions C1) and C2). However, they only use (T, N) at the transmitter (certainly they all use (T, N, L, Q) at the receiver), and do not enable the maximum delay-Doppler diversity provided by the doubly selective channel. Note that for time-flat frequency-selective channels, our transceiver specializes to the transceiver of [27], whereas for time-selective frequency-flat channels our transceiver specializes to the transceiver of [14]. The work presented in [19], finally, uses the BEM of (3) to develop channel estimation and equalization algorithms for a *single-user* system.

Existence: The proposed transceiver is based on the design of a sextuple (T, N, L, Q, K, P) that satisfies the conditions C1)–C3). Such a sextuple will be referred to as an admissible sextuple. Rewriting condition C3) as

$$Q = \frac{UP(KT+LT)Q/(NT)}{1-2U(KT+LT)Q/(NT)}$$

and observing that $\min\{LT\} = \tau_{\max}$ and $\min\{Q/(NT)\} = f_{\max}$, it is clear that a necessary condition for the existence of an admissible sextuple (T, N, L, Q, K, P) is $1 > 2U\tau_{\max}f_{\max}$. We call $S := 2U\tau_{\max}f_{\max}$ the *multiuser channel spread factor*, which is a generalization of the well-known single-user channel spread factor (product of delay and Doppler spread) [9]. Hence, $S < 1$ basically means that the multiuser channel has to be *underspread*, which intuitively speaking ensures that the number of equations is greater than the number of unknowns, when we want to estimate the doubly selective multiuser channel via training (see also [9]).

User Efficiency: We define the user efficiency as the ratio of the number of users U over the spreading gain $\mathcal{G} = N/M$

$$\mathcal{E} = \frac{U}{\mathcal{G}} = \frac{PK}{(P+2Q)(K+L)}.$$

Rewriting the user efficiency as

$$\mathcal{E} = \frac{KT}{KT+LT} - 2UKTQ/(NT)$$

and observing that $\min\{LT\} = \tau_{\max}$ and $\min\{Q/(NT)\} = f_{\max}$, it can be shown that the maximum user efficiency of the proposed transceiver is given by

$$\mathcal{E}_{\max} = \left(1-\sqrt{2U\tau_{\max}f_{\max}}\right)^2 = \left(1-\sqrt{S}\right)^2.$$

Remarkably, while in purely time- or frequency-selective channels the proposed transceiver can reach a maximum spectral efficiency arbitrarily close to 1, this is not possible anymore in doubly selective channels. However, for underspread channels with $S \ll 1$, which does not necessarily mean that we can neglect the time and/or frequency selectivity, the proposed transceiver can still accommodate close to $\mathcal{G}$ users.

Special Cases: In order to better understand what kind of signals are transmitted, let us focus on two special cases: $\boldsymbol{c}_u = \boldsymbol{i}_U[u]$ and $\boldsymbol{c}_u = \boldsymbol{f}_U[u]$. When $\boldsymbol{c}_u = \boldsymbol{i}_U[u]$, it can be shown that

$$\boldsymbol{x}_u[i] = \sum_{p=0}^{P-1}\sum_{k=0}^{K-1}\left(\boldsymbol{f}^*_{U(P+2Q)}[u(P+2Q)+p+Q] \otimes \boldsymbol{i}_{K+L}[k]\right)[\boldsymbol{s}_u[i]]_{pK+k}$$

$$\boldsymbol{F}_N\boldsymbol{x}_u[i] = \sum_{p=0}^{P-1}\sum_{k=0}^{K-1}\alpha_{u,p,k}\left(\boldsymbol{f}_{K+L}[k] \otimes \boldsymbol{i}_{U(P+2Q)}[u(P+2Q)+p+Q]\right)[\boldsymbol{s}_u[i]]_{pK+k}$$

where

$$\alpha_{u,p,q} := \exp(-j2\pi[u(P+2Q)+p+Q]k/N)$$

from which it is clear that the symbol $[\boldsymbol{s}_u[i]]_{pK+k}$ is modulated on a waveform that occupies a $(K+L)\times U(P+2Q)$ lattice in the time–frequency plane, as depicted in Fig. 4 (frequency-division multiple access (FDMA)-like transmission). When $\boldsymbol{c}_u = \boldsymbol{f}_U[u]$, it can be shown that

$$\boldsymbol{x}_u[i] = \sum_{k=0}^{K-1}\sum_{p=0}^{P-1}\beta_{u,p}\left(\boldsymbol{f}^*_{P+2Q}[p+Q] \otimes \boldsymbol{i}_{U(K+L)}[u(K+L)+k]\right)[\boldsymbol{s}_u[i]]_{pK+k}$$

$$\boldsymbol{F}_N\boldsymbol{x}_u[i] = \sum_{k=0}^{K-1}\sum_{p=0}^{P-1}\beta_{u,p}\gamma_{u,p,k}\left(\boldsymbol{f}_{U(K+L)}[u(K+L)+k] \otimes \boldsymbol{i}_{P+2Q}[p+Q]\right)[\boldsymbol{s}_u[i]]_{pK+k}$$

where

$$\beta_{u,p} := \exp(j2\pi u(p+Q)/[U(P+2Q)])$$

and

$$\gamma_{u,p,k} := \exp(-j2\pi[u(K+L)+k](p+Q)/N)$$

from which it is clear that the symbol $[\boldsymbol{s}_u[i]]_{pK+k}$ is modulated on a waveform that occupies a $U(K+L)\times(P+2Q)$ lattice in the time–frequency plane, as depicted in Fig. 4 (time-division multiple access (TDMA)-like transmission). In the above FDMA-like and TDMA-like transmissions, the set of lattices corresponding to a single user forms a set of bands in the frequency or time dimension, respectively. But every symbol in each user's block $\boldsymbol{s}_u[i]$ "rides on" a lattice that is present in multiple time–frequency boxes in Fig. 4. Other sets of orthogonal code vectors, e.g., the set of Walsh–Hadamard code vectors, lead to CDMA-like transmissions, which have the potential to be more robust against noise/interference that is narrow in time and/or frequency. In this case, the symbol $[\boldsymbol{s}_u[i]]_{pK+k}$ is modulated on a waveform that occupies a $U(K+L)\times U(P+2Q)$ lattice in the time–frequency plane. The symbol $[\boldsymbol{s}_u[i]]_{pK+k}$ is now present in every time–frequency box depicted in Fig. 4 (in contrast to the FDMA-like and TDMA-like transmissions). Hence, the set of KP lattices corresponding to a single user covers the entire time–frequency plane (up to the guard bands in time and frequency). This means that the sets of lattices corresponding to different users completely overlap in time and frequency, yet the mutual orthogonality among users is preserved at the receiver due to the orthogonality of the set $\{\boldsymbol{c}_u\}_{u=0}^{U-1}$.

Backward Compatibility With DS-CDMA: It can be shown that the block spreading by $\boldsymbol{C}_u$ and the block despreading by $\boldsymbol{D}_u$ can be implemented based on conventional symbol spreading and despreading combined with (I)FFT operations and interleaving, as depicted in Fig. 6 (the interleaver model is

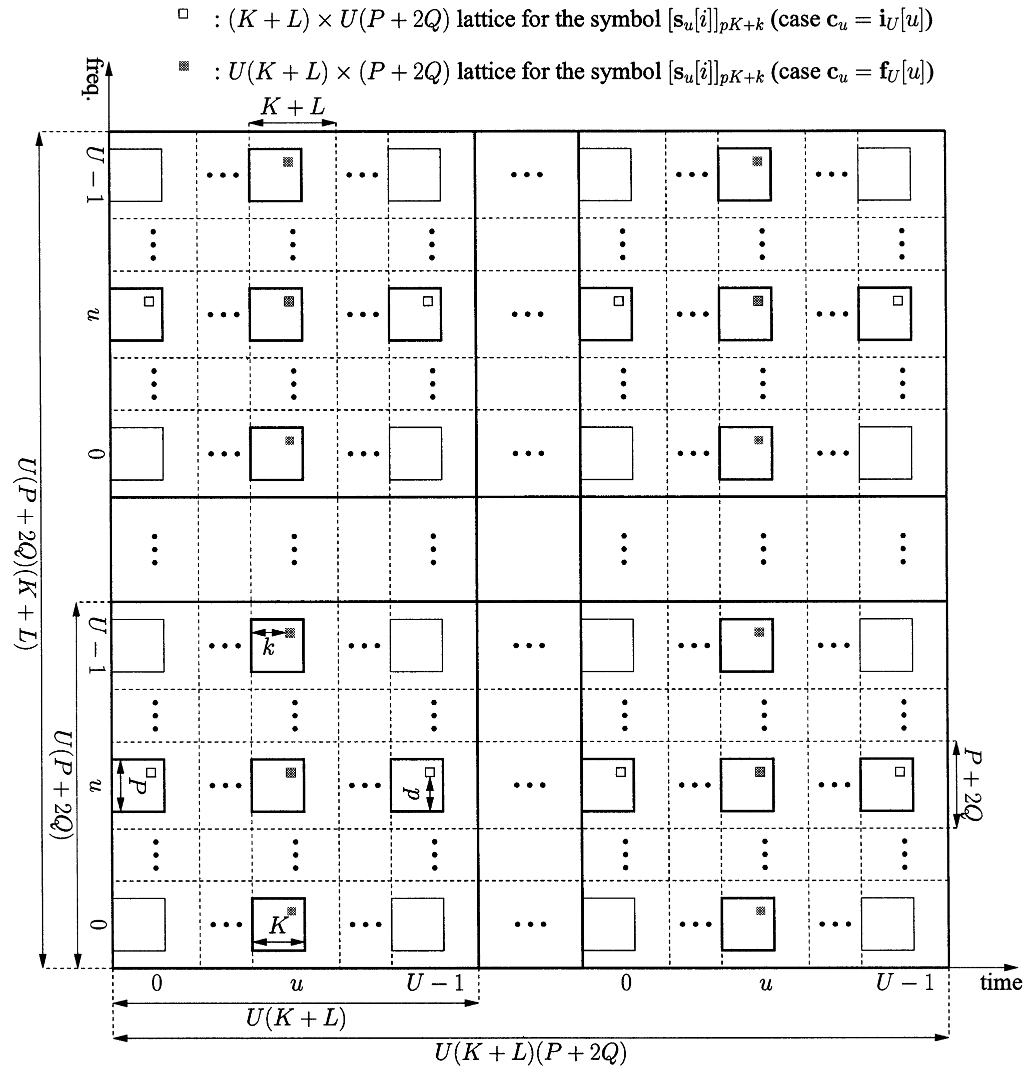

Fig. 4. Lattice structure for the symbol $[\boldsymbol{s}_u[i]]_{pK+k}$ (cases $\boldsymbol{c}_u = \boldsymbol{i}_U[u]$ and $\boldsymbol{c}_u = \boldsymbol{f}_U[u]$).

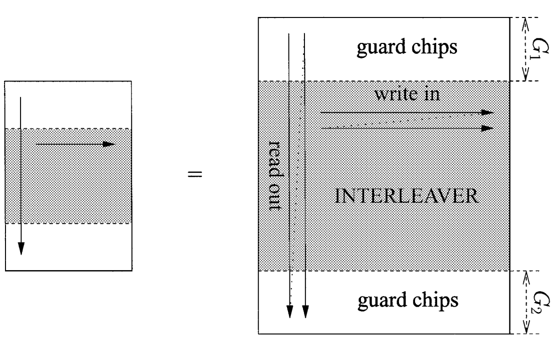

Fig. 5. Interleaver model.

depicted in Fig. 5). Hence, the proposed transceiver is backward compatible with DS-CDMA. Note that for time-flat frequency-selective channels this structure specializes to the one in [27, Fig. 4]. The above implementation can save computations at the base station, where all users are processed jointly. Implementing the block spreading and despreading at the base station as matrix–vector multiplications, the base station's spreading and despreading complexities are $\mathcal{O}\{U^2(P+2Q)PK\}$ and $\mathcal{O}\{U^2(P+2Q)^2(K+L)\}$ per block, respectively. However, implementing the block spreading and despreading at the base station as in Fig. 6, the (inverse) FFT ((I)FFT) operation can be shared among all users to save computations. The base station's spreading and despreading complexities then reduce to $\mathcal{O}\{U(P+2Q)\log_2(U(P+2Q))K\} + \mathcal{O}\{U^2PK\}$ and $\mathcal{O}\{U(P+2Q)\log_2(U(P+2Q))(K+L)\} + \mathcal{O}\{U^2(P+2Q)(K+L)\}$ per block, respectively. Note that the terms $\mathcal{O}\{U^2PK\}$ and $\mathcal{O}\{U^2(P+2Q)(K+L)\}$, which correspond to the conventional symbol spreading and despreading, vanish when $\boldsymbol{c}_u = \boldsymbol{i}_U[u]$.

Error Control Coding: Outer error control coding is certainly applicable prior to spreading, and will improve the overall system performance in practice, at the expense of information rate loss that can be afforded by the underlying application. As for information rate limits, neither the (non)coherent capacity (average or outage) of doubly selective channels, nor the transmit-waveforms approaching capacity are available. Albeit important and challenging, their investigation goes well beyond the scope of this paper. For related issues, the reader is referred to [17], [18].

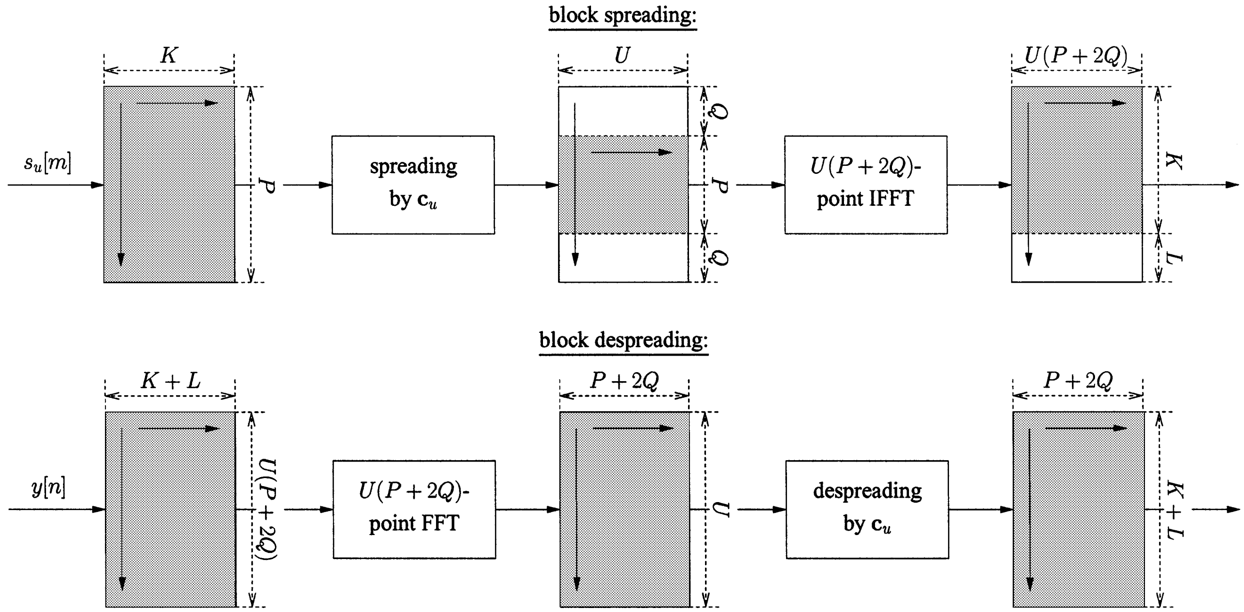

Fig. 6. Implementation of the block spreading by $\boldsymbol{C}_u$ (upper part) and the block despreading by $\boldsymbol{D}_u$ (lower part) based on interleaving.

VI. Conclusion

Relying on a BEM for doubly selective channels, we have developed a channel-independent block spreading scheme that preserves mutual orthogonality among single-cell users at the receiver. This alleviates the need for complex multiuser detection, and enables separation of the desired user by a simple code-matched channel-independent block despreading scheme that is ML optimal under the BEM plus white Gaussian noise assumption on the channel. In addition, our block spreading enables the maximum delay-Doppler diversity per user, when the BEM coefficients are Gaussian distributed. Issues like links with existing multiuser transceivers, existence, user efficiency, special cases, backward compatibility with DS-CDMA, and error control coding, have been briefly discussed.

Appendix A
Proof of (10)

First, $\boldsymbol{H}^{(0)}_{N,u,q}[i]$ can be expressed as [27]

$$\boldsymbol{H}^{(0)}_{N,u,q}[i] = \boldsymbol{I}_{U(P+2Q)} \otimes \boldsymbol{H}^{(0)}_{K+L,u,q}[i] + \boldsymbol{J}^{(0)}_{U(P+2Q),1} \otimes \boldsymbol{H}^{(1)}_{K+L,u,q}[i]. \quad (15)$$

Using (15) and the fact that $\boldsymbol{H}^{(1)}_{K+L,u,q}[i]\boldsymbol{T}_1 = \mathbf{0}_{(K+L)\times K}$, we then obtain

$$\begin{aligned}
&\boldsymbol{H}^{(0)}_{N,u,q}[i]\boldsymbol{C}_u \\
&= \boldsymbol{H}^{(0)}_{N,u,q}[i]\left\{\left[\boldsymbol{F}^H_{U(P+2Q)}(\boldsymbol{c}_u \otimes \boldsymbol{T}_2)\right] \otimes \boldsymbol{T}_1\right\} \\
&= \Big(\boldsymbol{I}_{U(P+2Q)} \otimes \boldsymbol{H}^{(0)}_{K+L,u,q}[i] \\
&\quad + \boldsymbol{J}^{(0)}_{U(P+2Q),1} \otimes \boldsymbol{H}^{(1)}_{K+L,u,q}[i]\Big) \\
&\quad \cdot \left\{\left[\boldsymbol{F}_{U(P+2Q)}(\boldsymbol{c}_u \otimes \boldsymbol{T}_2)\right] \otimes \boldsymbol{T}_1\right\} \\
&= \left[\boldsymbol{F}^H_{U(P+2Q)}(\boldsymbol{c}_u \otimes \boldsymbol{T}_2)\right] \otimes \boldsymbol{H}_{u,q}[i] + \mathbf{0}_{N\times M} \\
&= \left\{\left[\boldsymbol{F}^H_{U(P+2Q)}(\boldsymbol{c}_u \otimes \boldsymbol{T}_2)\right] \otimes \boldsymbol{I}_{K+L}\right\}(\boldsymbol{I}_P \otimes \boldsymbol{H}_{u,q}[i]).
\end{aligned}$$

This concludes the proof of (10).

Appendix B
Proof of (11)

First, let us introduce the notation $\boldsymbol{Z}_{N,q}$, which represents the $N \times N$ circulant matrix with

$$[\boldsymbol{Z}_{N,q}]_{n,n'} = \delta[(n - n' - q) \bmod N]$$

It can then be shown that

$$\begin{aligned}
&\boldsymbol{\Lambda}_N\left(\frac{q}{N}\right)\left\{\left[\boldsymbol{F}^H_{U(P+2Q)}(\boldsymbol{c}_u \otimes \boldsymbol{T}_2)\right] \otimes \boldsymbol{I}_{K+L}\right\} \\
&= \left(\boldsymbol{\Lambda}_{U(P+2Q)}\left(\frac{q}{U(P+2Q)}\right) \otimes \boldsymbol{\Delta}_q\right) \\
&\quad \cdot \left\{\left[\boldsymbol{F}^H_{U(P+2Q)}(\boldsymbol{c}_u \otimes \boldsymbol{T}_2)\right] \otimes \boldsymbol{I}_{K+L}\right\} \\
&= \left[\boldsymbol{\Lambda}_{U(P+2Q)}\left(\frac{q}{U(P+2Q)}\right)\boldsymbol{F}^H_{U(P+2Q)}(\boldsymbol{c}_u \otimes \boldsymbol{T}_2)\right] \otimes \boldsymbol{\Delta}_q \\
&= \left[\boldsymbol{F}^H_{U(P+2Q)}\boldsymbol{Z}_{U(P+2Q),q}(\boldsymbol{c}_u \otimes \boldsymbol{T}_2)\right] \otimes \boldsymbol{\Delta}_q \quad (16)
\end{aligned}$$

where the last equality comes from the fact that

$$\boldsymbol{\Lambda}_{U(P+2Q)}\left(\frac{q}{U(P+2Q)}\right)$$

cyclically shifts the columns of $\boldsymbol{F}^H_{U(P+2Q)}$ with q positions to the left. Next, $\boldsymbol{Z}_{U(P+2Q),q}$ can be expressed as

$$\boldsymbol{Z}_{U(P+2Q),q} = \boldsymbol{Z}_{U,-1} \otimes \boldsymbol{J}^{(-1)}_{P+2Q,q} + \boldsymbol{I}_U \otimes \boldsymbol{J}^{(0)}_{P+2Q,q} + \boldsymbol{Z}_{U,1} \otimes \boldsymbol{J}^{(1)}_{P+2Q,q}. \quad (17)$$

Using (17) and the fact that

$$\boldsymbol{J}^{(-1)}_{P+2Q,q}\boldsymbol{T}_2 = \boldsymbol{J}^{(1)}_{P+2Q,q}\boldsymbol{T}_2 = \mathbf{0}_{(P+2Q)\times P}$$

we then obtain

$$\begin{aligned}&\boldsymbol{Z}_{U(P+2Q),\,q}(\boldsymbol{c}_u \otimes \boldsymbol{T}_2)\\ &\quad= \Big(\boldsymbol{Z}_{U,\,-1}\otimes \boldsymbol{J}^{(-1)}_{P+2Q,\,q} + \boldsymbol{I}_U \otimes \boldsymbol{J}^{(0)}_{P+2Q,\,q}\\ &\qquad + \boldsymbol{Z}_{U,\,1}\otimes \boldsymbol{J}^{(1)}_{P+2Q,\,q}\Big)(\boldsymbol{c}_u \otimes \boldsymbol{T}_2)\\ &\quad= \boldsymbol{0}_{U(P+2Q)\times P} + \boldsymbol{c}_u \otimes \boldsymbol{J}_q + \boldsymbol{0}_{U(P+2Q)\times P}. \end{aligned} \tag{18}$$

Using (18), we can simplify (16) as

$$\begin{aligned}&\boldsymbol{\Lambda}_N\left(\frac{q}{N}\right)\left\{\left[\boldsymbol{F}^H_{U(P+2Q)}(\boldsymbol{c}_u\otimes \boldsymbol{T}_2)\right]\otimes \boldsymbol{I}_{K+L}\right\}\\ &\quad= \left[\boldsymbol{F}^H_{U(P+2Q)}(\boldsymbol{c}_u\otimes \boldsymbol{J}_q)\right]\otimes \boldsymbol{\Delta}_q\\ &\quad= \left[\boldsymbol{F}^H_{U(P+2Q)}(\boldsymbol{c}_u\otimes \boldsymbol{I}_{P+2Q})\boldsymbol{J}_q\right]\otimes \boldsymbol{\Delta}_q\\ &\quad= \left\{\left[\boldsymbol{F}^H_{U(P+2Q)}(\boldsymbol{c}_u\otimes \boldsymbol{I}_{P+2Q})\right]\otimes \boldsymbol{I}_{K+L}\right\}(\boldsymbol{J}_q\otimes \boldsymbol{\Delta}_q)\\ &\quad= \boldsymbol{D}_u(\boldsymbol{J}_q\otimes \boldsymbol{\Delta}_q).\end{aligned}$$

This concludes the proof of (11).

REFERENCES

[1] S. Bhashyam, A. M. Sayeed, and B. Aazhang, "Time-selective signaling and reception for communication over multipath fading channels," *IEEE Trans. Commun.*, vol. 48, pp. 83–94, Jan. 2000.

[2] J. W. Brewer, "Kronecker products and matrix calculus in system theory," *IEEE Trans. Circuits Syst.*, vol. CAS-25, pp. 772–781, Sept. 1978.

[3] J. K. Cavers, *Mobile Channel Characteristics*. Norwell, MA: Kluwer, 2000.

[4] A. Duel-Hallen, S. Hu, and H. Hallen, "Long-range prediction of fading channels," *IEEE Signal Processing Mag.*, pp. 62–75, May 2000.

[5] G. B. Giannakis, Y. Hua, P. Stoica, and L. Tong, Eds., *Signal Processing Advances in Wireless & Mobile Communications: Trends in Single- and Multi-User Systems*. Upper Saddle River, NJ: Prentice-Hall, 2000, vol. 2.

[6] G. B. Giannakis and C. Tepedelenlioğlu, "Basis expansion models and diversity techniques for blind equalization of time-varying channels," *Proc. IEEE*, vol. 86, pp. 1969–1986, Oct. 1998.

[7] G. B. Giannakis, Z. Wang, A. Scaglione, and S. Barbarossa, "AMOUR-generalized multi-carrier transceivers for blind CDMA regardless of multipath," *IEEE Trans. Commun.*, vol. 48, pp. 2064–2076, Dec. 2000.

[8] W. C. Jakes, Ed., *Microwave Mobile Communications*. New York: Wiley, 1974.

[9] T. Kailath, "Measurements on time-variant communication channels," *IEEE Trans. Inform. Theory*, vol. IT-8, pp. S229–S236, Sept. 1962.

[10] G. Leus and M. Moonen, "MUI-free receiver for a synchronous DS-CDMA system based on block spreading in the presence of frequency-selective fading," *IEEE Trans. Signal Processing*, vol. 48, pp. 3175–3188, Nov. 2000.

[11] X. Ma and G. B. Giannakis, "Designing maximum multipath-Doppler diversity transmissions over time- and frequency-selective wireless channels," in *Proc. 39th Allerton Conf.*, Monticello, IL, Oct. 2001, pp. 682–691.

[12] M. Martone, "Wavelet-based separating kernels for array processing of cellular DS/CDMA signals in fast fading," *IEEE Trans. Commun.*, vol. 48, pp. 979–995, June 2000.

[13] E. N. Onggosanusi, A. M. Sayeed, and B. D. Van Veen, "Canonical space-time processing for wireless communications," *IEEE Trans. Commun.*, vol. 48, pp. 1669–1680, Oct. 2000.

[14] S. Barbarossa, M. Pompili, and G. B. Giannakis, "Channel-independent synchronization of orthogonal frequency division multiple access systems," *IEEE J. Select. Areas Commun.*, vol. 20, pp. 474–486, Feb. 2002.

[15] A. M. Sayeed and B. Aazhang, "Joint multipath-doppler diversity in mobile wireless communications," *IEEE Trans. Commun.*, vol. 47, pp. 123–132, Jan. 1999.

[16] A. M. Sayeed, A. Sendonaris, and B. Aazhang, "Multiuser detection in fast-fading multipath environments," *IEEE J. Select. Areas Commun.*, vol. 16, pp. 1691–1701, Dec. 1998.

[17] S. Shamai (Shitz) and A. D. Wyner, "Information-theoretic considerations for symmetric, cellular, multiple-acess fading channels—Part I," *IEEE Trans. Inform. Theory*, vol. 43, pp. 1877–1894, Nov. 1997.

[18] ——, "Information-theoretic considerations for symmetric, cellular, multiple-acess fading channels—Part II," *IEEE Trans. Inform. Theory*, vol. 43, pp. 1895–1911, Nov. 1997.

[19] C. Tepedelenlioğlu and G. B. Giannakis, "Transmitter redundancy for blind estimation and equalization of time- and frequency-selective channels," *IEEE Trans. Signal Processing*, vol. 48, pp. 2029–2043, July 2000.

[20] T. A. Thomas and F. W. Vook, "Multi-user frequency-domain channel identification, interference suppression, and equalization for time-varying broadband wireless communications," in *Proc. Sensor Array and Multichannel Signal Processing Workshop*, Cambridge, MA, Mar. 2000, pp. 444–448.

[21] ——, "Quasistatic antenna array processing for rapidly time-varying channels," in *Proc. Int. Conf. Acoustics Speech, and Signal Processing*, Salt Lake City, UT, May 2001, pp. 2977–2980.

[22] M. K. Tsatsanis and G. B. Giannakis, "Modeling and equalization of rapidly fading channels," *Int. J. Adaptive Control and Signal Processing*, vol. 10, no. 2/3, pp. 159–176, Mar. 1996.

[23] S. Verdú, *Multiuser Detection*. Cambridge, U.K.: Cambridge Univ. Press, 1998.

[24] Z. Wang and G. B. Giannakis, "Wireless multicarrier communications: Where Fourrier meets Shannon," *IEEE Signal Processing Mag.*, pp. 29–48, May 2000.

[25] G. W. Wornell, "Spread-signature CDMA: Efficient multiuser communication in the presence of fading," *IEEE Trans. Inform. Theory*, vol. 41, pp. 1418–1438, Sept. 1995.

[26] ——, "Spread-response precoding for communication over fading channels," *IEEE Trans. Inform. Theory*, vol. 42, pp. 488–501, Mar. 1996.

[27] S. Zhou, G. B. Giannakis, and C. Le Martret, "Chip-interleaved block-spread code division multiple access," *IEEE Trans. Commun.*, vol. 50, pp. 235–248, Feb. 2002.

[28] Z. Zvonar and D. Brady, "Linear multipath-decorrelating receivers for CDMA frequency-selective fading channels," *IEEE Trans. Commun.*, vol. 44, pp. 650–653, June 1996.